EU contract number RII3-CT-2003-506395 CARE-Report-2007-038-SRF

SRF

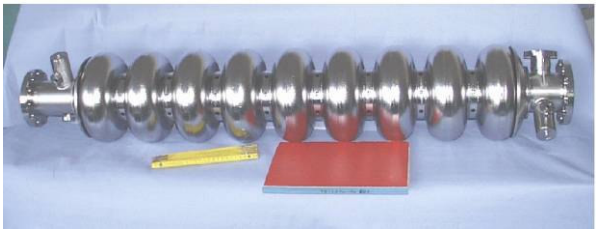

WP11 (Beam diagnostics)

The Cold Re-entrant BPM

C. Simon, M. Luong, S. Chel, O. Napoly, J. Novo, D. Roudier
CEA, Saclay, France
N. Rouvière
CNRS, Orsay, France
N. Baboi, D. Noelle, N. Mildner
DESY, Hamburg, Germany

Abstract

The beam-based alignment and feedback systems, essential for the future colliders, need high resolution Beam Position Monitors (BPM). In the framework of the European CARE/SRF program, the task of CEA/DSM/DAPNIA covers the design, the fabrication and the beam test of these BPMs in collaboration with DESY. The objective of this program is the production of a BPM that has a resolution five times better than the existing device while maintaining a high time resolution and which can be used in a clean environment at cryogenic temperature. Two prototypes of this monitor, based on a radio-frequency cavity with a beam pipe diameter of 78 mm, are installed on the Free Electron LASer in Hamburg (FLASH).

Introduction

This paper presents the evolution of a re-entrant cavity beam position monitor (BPM), developed by the CEA Saclay in collaboration with DESY, in the framework of the CARE/SRF European program.

This BPM is composed of a radio-frequency re-entrant cavity with a beam pipe diameter of 78 mm, four feedthroughs and a signal processing electronics. The mechanical and signal processing designs are a compromise to get a high position resolution and a high time resolution. It is specially designed to be connected to superconducting cavities, environment where dust contamination has to be avoided.

The Free electron LASer in Hamburg (FLASH) linac at DESY was known as the VUV-Free Electron Laser (VUV-FEL) and it is also used as a test facility for the X-ray Free Electron Laser (XFEL) and for the International Linear Collider (ILC) study under the name TESLA Test Facility-Phase 2 (TTF2).

A first prototype of a re-entrant BPM has delivered measurements at 2K inside the first cryomodule (ACC1) on the FLASH linac. The performances of this BPM are analyzed and the limitations of this existing system clearly identified. Finally, the solution which requires a new design for both the BPM cavity and the signal processing electronics was been adopted. With this new BPM, the position resolution is expected to be better than 10 µm and the time resolution is high enough to ensure bunch to bunch measurement for XFEL or ILC. This second prototype has been qualified with beam in a warm section of the FLASH accelerator, achieving 4 µm resolution over a dynamic range of ± 5 mm.

This paper describes the theoretical performances of this system and the measurements carried out with beam on the FLASH linac.

Re-entrant cavity BPM Design

Coaxial re-entrant cavity has been chosen for the beam orbit measurement because of its mechanical simplicity and excellent resolution. This cavity is composed of a mechanical structure which consists in three distinct regions: beam tube (I), gap (II) and coaxial cylinder (III) (Fig. 1), with four orthogonal feedthroughs. It has a small size and a cylindrical symmetry which allows a high precision of the machining. Arranged around the beam pipe the cavity forms a coaxial line which is short circuited at the downstream end [1].

The cavity is fabricated with stainless steel as compact as possible. Its length is 170 mm to satisfy the constraints imposed by the cryomodule. The aperture of the cavity is 78 mm (aperture of an TTF cavity), the gap (g) is 8 mm and the length of the coaxial cylinder is 50 mm as shown Fig.1. The fixing of the antenna tips to the inner diameter of the cavity over coupled the cavity.

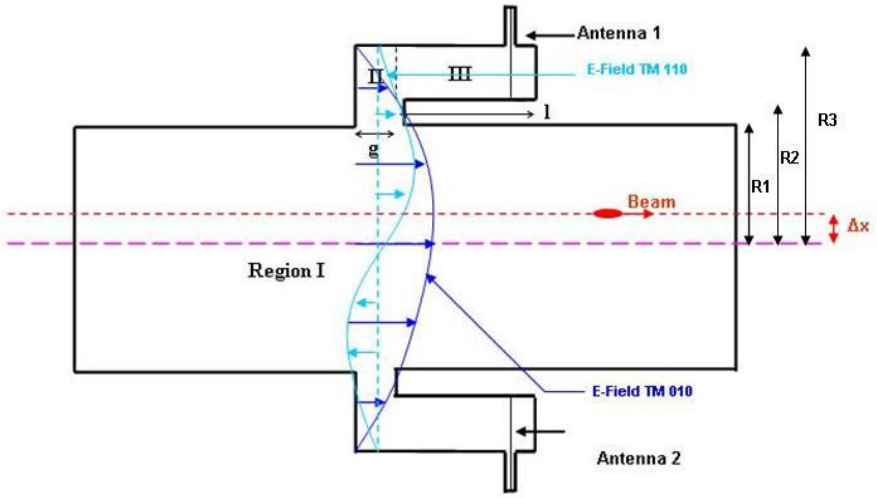

l	50 mm
g	8 mm
R1	39 mm
R2	41.5 mm
R3	49.5 mm

FIGURE 1: Geometry of the re-entrant cavity BPM.

Passing through this cavity, the beam excites some electro-magnetic fields (resonant modes), which are coupled by four feedthroughs to the outside: two of them determine the horizontal position (X position) and two others the vertical position (Y position).

The main radio-frequency modes excited by the beam in the cavity are monopole and dipole modes. The signal voltage of the monopole mode (type TM010) is proportional to beam intensity and does not depend on the beam position. This signal will be used for the normalization. The dipole mode (type TM110) voltage is proportional to the intensity and to the distance of the beam from the centre axis of the monitor. The higher order modes are damped much more strongly so their contribution is negligible and the linearity of the measurement is ensured.

As shown on the Fig. 2, the beam position (X and Y) can be calculated by the ratio of the difference of voltages V1 - V3 and V2 - V4 which correspond to the voltage of the dipole field with the sum V1 + V3 and V2 + V4 which correspond to the voltage of the monopole filed in the both axis.

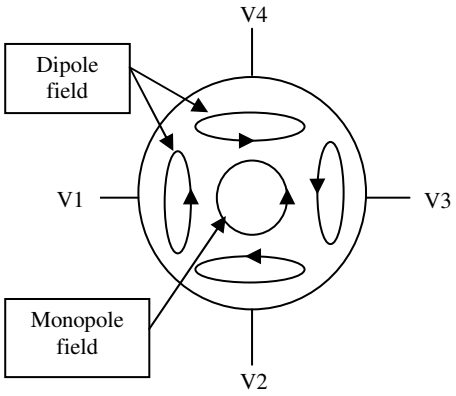

V1 = V(monopole) + V(dipole)
V2 = V(monopole) + V(dipole)
V3 = V(monopole) - V(dipole)
V4 = V(monopole) - V(dipole)

X = L (V1 - V3) / (V1 + V3)
Y = L (V2 – V4) / (V2 + V4)
L = constant

FIGURE 2: Resonant modes of the re-entrant cavity.

Two re-entrant BPMs are installed on FLASH linac at DESY. The first is operated at cryogenic temperature inside the cryomodule, in an environment where dust particle contamination has to be avoided. The second is installed on a warm part of the linac to be qualified with beam.

BPM installed in a cryomodule

An existing BPM designed for the TTF injector was installed in a cryomodule to carry out some measurements with beam [2].

Cavity BPM

The re-entrant cavity (Fig.3) was installed in 2004 at cryogenic temperature inside a cryomodule (ACC1) on the FLASH linac.

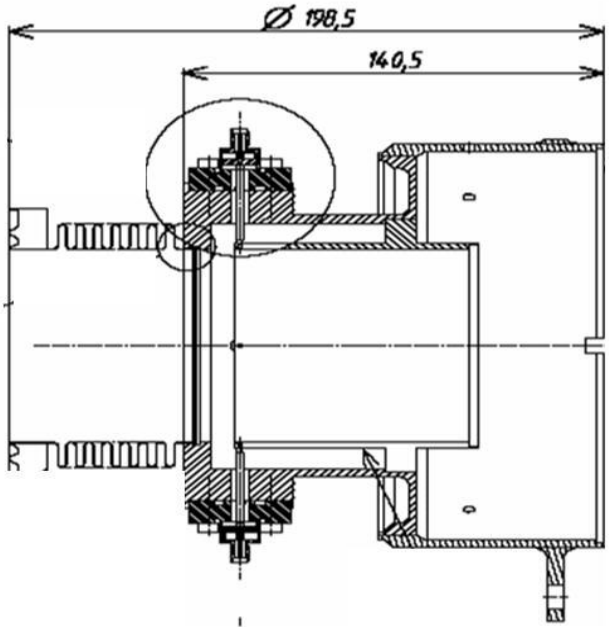

Fig.3: Drawing of the re-entrant cavity installed in the cryomodule

Figure 4 shows this monitor before insertion into the cryomodule.

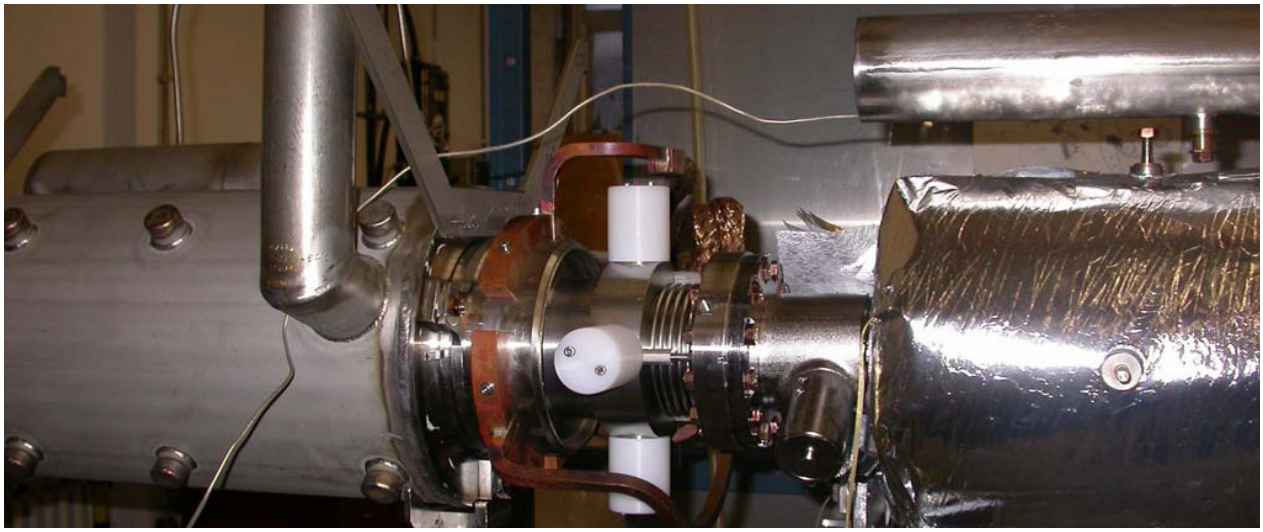

FIGURE 4: BPM installed in a cryomodule with four feedthroughs protected by plastic cylinders during mounting.

The RF characteristics of this cavity (eigenmodes frequencies, quality factors and longitudinal R/Q) are calculated with the HFSS code provided by Ansoft Corporation. The results are given in Table 1.

TABLE 1. RF characteristics of the BPM installed in the cryomodule.

Eigen modes	**F (GHz)**	**Q_{ext}**	**R/Q_l (Ω) at 5 mm**	**R/Q_l (Ω) at 10 mm**
Monopole mode	1.58	2.15	20.2	20.4
Dipole mode	2.01	4.11	0.53	2.20
Quadrupole mode	2.25	0.97	0.01	0.01

The quality factors Q are determined by HFSS with matched feedthroughs in eigen solver mode. With Matlab and the HFSS calculator, the R/Q ratio was computed (R: the Shunt impedance and Q: quality factor) with the following formulae:

$$\frac{R}{Q} = \frac{V^2}{2*\pi*f*W} \qquad (1)$$

with $V = \left| \int E(z)*e^{jkz}\,dz \right|$ where k= w/c and W is the stored energy in the mode $W = \left| \frac{\varepsilon_0}{2} \iiint E*E^* \right| d\tau$

Table 1 shows a coupling which is very high, the first monopole and dipole modes have respectively a quality factor Q = 2 and Q = 4. With those low values, the signals are spread out in spectrum, the distinguishing of monopole and dipole modes is not easy and the monopole signal is not, efficiently, rejected.

Signal processing

The beam position can be measured from the output voltage of a pair of feedthroughs mounted on the opposite sides of the cavity on both axes. Signals detected by the signal processing electronics extract the beam position (displacement) and deliver this information to the acquisition board. Due to the low external quality factor, the single bunch response of the cavity has to be broadened before its acquisition. The 8 MHz bandwidth of this filter defines the bandwidth of the system and determines the time resolution [3]. The signal processing uses a single stage down conversion to obtain Δ/Σ. The chosen measurement frequency, is 650 MHz. This frequency is a multiple of the repetition bunch frequency

(216.66 MHz) on the first TTF injector and is defined by a Bessel bandpass filter used in the signal processing electronics.

Two boxes compose the electronics of this BPM: the calibration box and the synchronous detection box (Fig. 5). A 180° hybrid junction, connected to each pair of opposite antennae with 33 m of semi-rigid cables, yields the sum and the difference of RF voltages proportional to the beam current and position. These RF signals are then filtered, amplified and demodulated with a synchronous detection. The sum signal is used as a local oscillator signal for the mixer. The acquisition is carried out either by standard COMET boards of the TTF control system, or by dedicated boards to other applications.

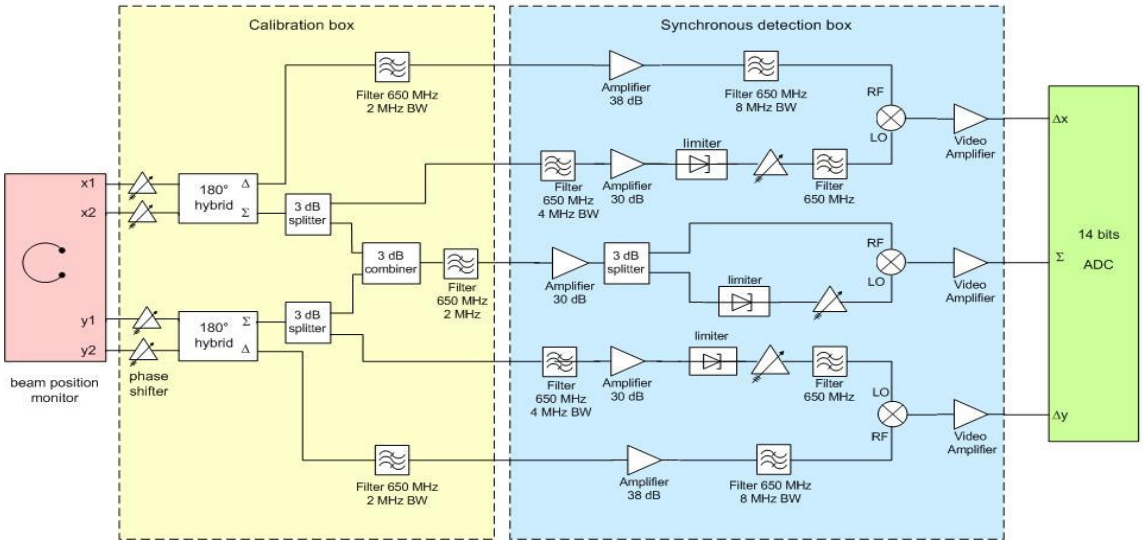

FIGURE 5: Signal processing electronics of the BPM installed in a cryomodule.

Beam tests on the BPM installed in the cryomodule

In March 2006, a calibration was carried out on the BPM installed in a FLASH cryomodule. It was operated in single bunch for these measurements which produced statistics and correlations. To calibrate this BPM called 9ACC1, the following method was used. The relative beam displacement at the BPM location was calculated in using a transfer matrix between steerers and BPM (made of drifts and accelerating cavities) for different values of drive current in the steerers:

$$\Delta x = R_{12} * \Delta x' \quad \text{(where } \Delta x\text{' is the beam angle at steerer).}$$

The HOM (Higher Order Mode) signals [4] from the closest cavity to the BPM installed in the cryomodule, were minimized thanks to beam steering. This minimization gave an estimation of the BPM centre. The beam tilt was neglected due to the closeness of BPM 9ACC1 to this cavity. An offset on Δx and Δy channels was added in the acquisition software to read a zero in this condition. Another calibration coefficient was computed from a linear fit of the predicted position to the measured position. The relative beam position is calculated for each steerer setting in using a transfer matrix between steerers and BPM made of drifts and accelerating cavities. With this calibration method, the re-entrant BPM showed a linear range about ± 1.5 mm before saturation due to amplifiers or analog to digital converters.

On the Fig.6, the plots of the predicted position vs. the position read by 9ACC1, on X and Y channels are presented. The nominal bunch charge is about 1 nC.

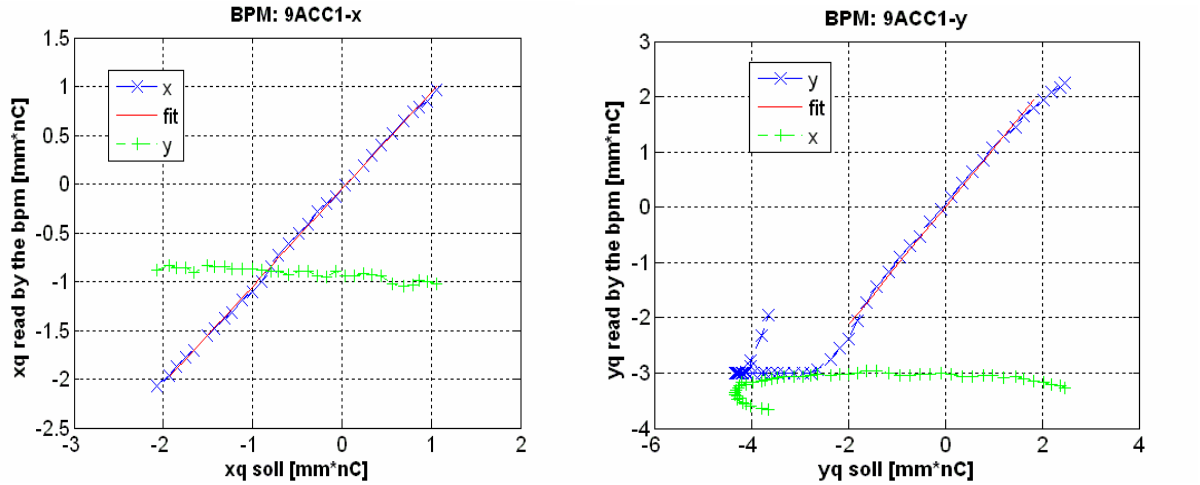

FIGURE 6: Position read by 9ACC1 vs. the predicted position in horizontal and vertical steering

The raw RMS resolution of the system directly measured by the standard deviation of the readings from 9ACC1 is around 50 µm on the X channel. In correlating the reading of the re-entrant BPM in one plane against the readings of all other BPMs in the same plane, the BPM resolution can be measured [5]. The beam jitter can be canceled and the position resolution can be estimated around 20 µm. On the Y channel, the resolution is around 30 µm after the beam jitter cancellation and around 70 µm as a raw measurement.

These results show the limitation of the system as shown with the theoretical results [6]. Moreover, due to the bandpass filter bandwidth, which is only 8 MHz, the bunch to bunch measurement on the FLASH linac and XFEL is impossible for this BPM system. A new design is therefore necessary to achieve a position resolution better than 10 µm and have the possibility to perform bunch to bunch measurements.

New design of the re-entrant BPM

To improve the time resolution and position resolution of the re-entrant BPM which has already proved its capability to be operated at cryogenic temperature inside the cryomodule, a new BPM system was designed.

Cavity BPM

The principle of the re-entrant cavity and the main dimensions of the cavity are kept: the gap 8 mm, the coaxial cylinder, 170 mm in length, 78 mm for the beam pipe and 152 mm in diameter as shown Fig. 7.

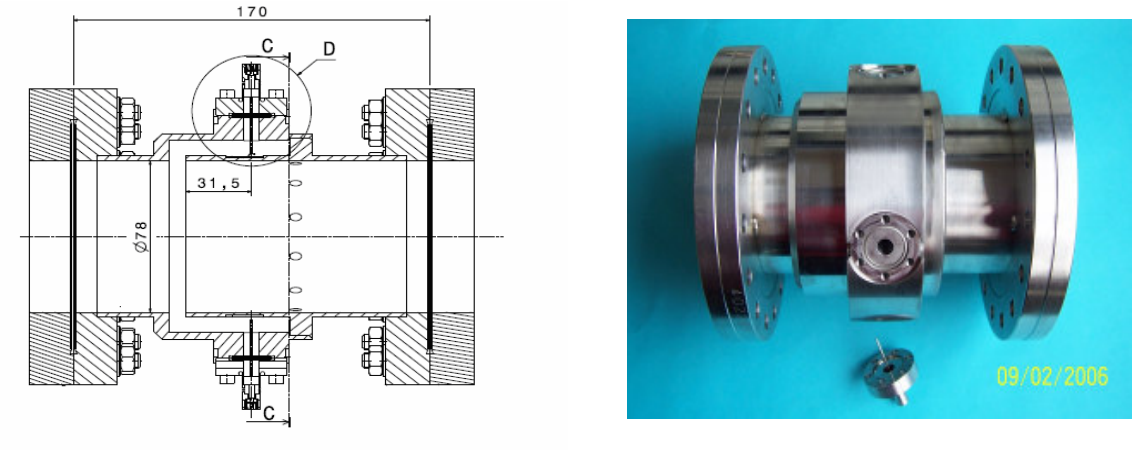

FIGURE 7: Drawing and photo of the modified BPM cavity.

The resolution better than 10 µm but also the mechanical feasibility of the structure determined the quality factors, Q, of the monopole and dipole modes. They are not able either to be too high to keep a time resolution around 10 ns or too low to have a resolution better than 10 µm.

In order to get a higher Q and therefore a longer signal in time without the need of a Bessel filter for signal shaping, the feedthroughs are moved 31.5 mm in the re-entrant part (Fig. 7). This antenna position reduces the magnetic loop coupling and increases the separation of the RF modes (monopole and dipole modes). Monopole and dipole signals have a better distinction and the rejection of the monopole signal is easier.

Antennas are assembled to the cavity by a conflat gasket (standard CF DN16) and fulfill the conditions of Ultra High Vacuum (UHV). Some copper-beryllium radio-frequency contacts were welded in the inner cylinder of the cavity to ensure electrical conduction between the feedthrough inner conductor and the cavity (Fig. 8), providing a magnetic coupling loop. In the past, a critical point concerned the feedthrough fragility; 50% of the feedthroughs had to be rejected. With this new design, the machining of feedthroughs is simpler and the final product more robust. Several cryogenic and vacuum tests (thermal shock) were carried out on the RF feedthroughs with success.

One of the biggest problems on the cavity installed in the cryomodule was the cleaning. As the BPM is designed to be used in a clean environment, twelve holes of 5 mm diameter are drilled at the end of the re-entrant part for more effective cleaning. Cleaning tests were successfully performed at DESY and validated the system for the cleaning.

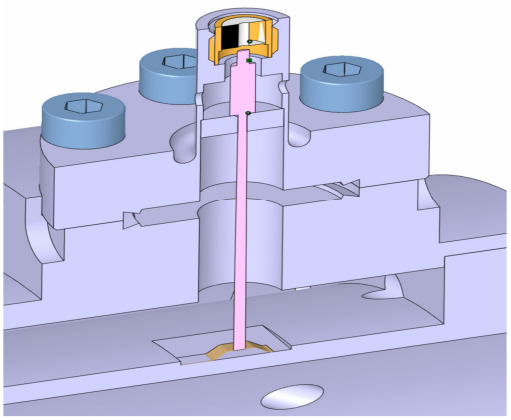

FIGURE 8: Design of the new feedthrough

The resonant cavity is, first, simulated with the software HFSS (Ansoft) to determine its frequencies, quality factors and R/Q. The RF measurements, presented in Table 2, compare some computed quantities to measured values. Figure 9 shows some electrical field plots for the monopole and dipole modes.

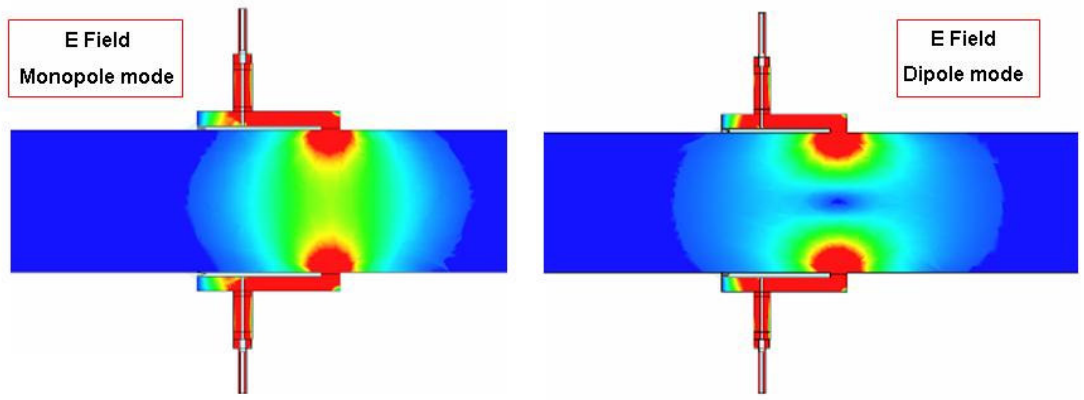

FIGURE 9: Electrical fields for the monopole and dipole modes

Spring 2006, during the maintenance time, the re-entrant BPM was installed in a warm part in the FLASH linac (Fig. 10) at DESY.

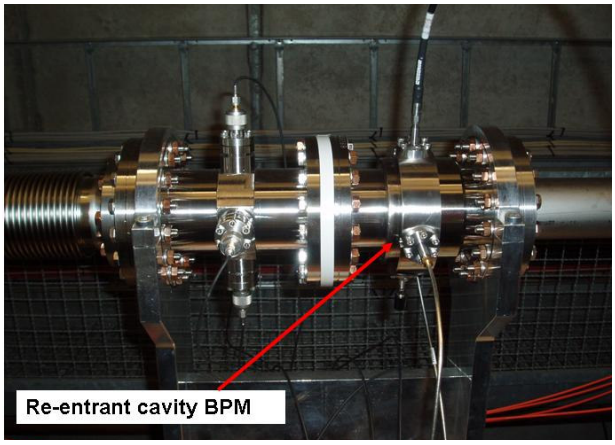

FIGURE 10: Re-entrant cavity BPM installed in the FLASH linac

After this mounting, the first RF measurements were carried out on the cavity BPM. The RF measurements, presented in Table 2, provide a comparison that gives information on the sensitivity of the RF characteristics to the machining, mounting and operating environments.

TABLE 2. RF characteristics of the new re-entrant BPM.

Eigen modes	**F (MHz)**		**Q_{ext}**		**R/Q_l (Ω) 5 mm offset**	**R/Q_l (Ω) 10 mm offset**
	Calculated	Measured	Calculated	Measured	Calculated	Calculated
Monopole mode	1250	1255	22.95	23.8	12.9	12.9
Dipole mode	1719	1724	50.96	59	0.27	1.15

The monopole and dipole modes are around 1.25 GHz and 1.72 GHz and the quality factors are quite low. The others modes of the cavity which have an eigen frequency higher than the beam pipe TE11 mode cut off frequency (2.25 GHz) are damped. Their contribution is negligible and the linearity of the measurement is ensured.

The reflection measurement on each pick up gives nearly the same results with only ±0.07 dB. The four pickups mounted on the BPM are therefore quite identical.

Each dipole mode orthogonal polarization was measured and shows slightly different eigenfrequencies; the relative difference is, however, less than 2 per 1000. Furthermore, the perfect polarization orthogonality is lost. Due to the finite tolerances in machining, welding and mounting, some small distortions of cavity symmetry are generated. A displacement of the beam in the 'x' direction gives not only a reading in that direction but also a non-zero reading in the orthogonal direction 'y' (Fig. 11).

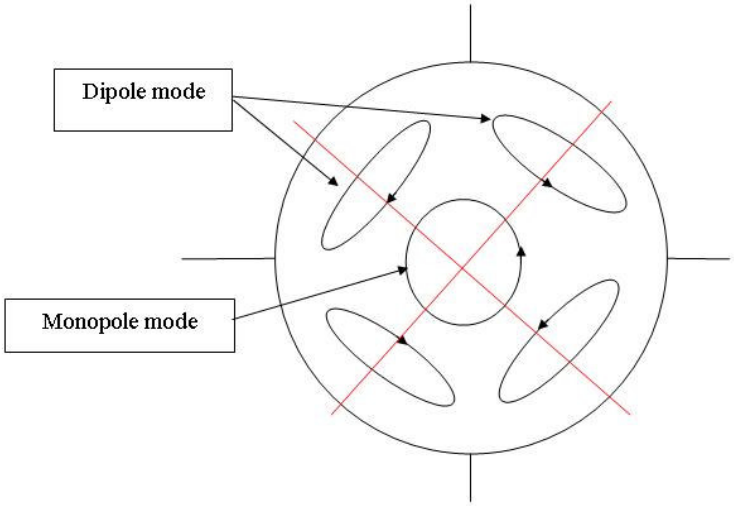

FIGURE 11: Cross-talk illustration

This asymmetry is called cross talk. Cross-talk isolation measurements are performed on the re-entrant cavity with a network analyzer. The transmission is first measured between two opposite antennas, the two other antennas are terminated with a 50 Ω load. In this configuration, the monopole and dipole modes are excited as displayed in the Fig. 12. At the dipole frequency (1.72 GHz), the transmission level was measured around -0.8 dB.

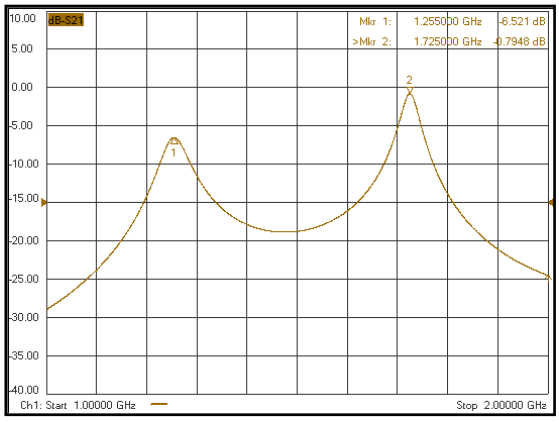

FIGURE 12. Monopole and dipole transmission measured by the network analyzer

For the second configuration, the signal transmission is measured between antennas positioned at 90° through a 180° hybrid coupler as shown in Fig. 13. The corresponding transmissions are displayed in Fig. 14. From those measurements, the cross-talk isolation value is estimated about 41 dB measured in laboratory instead of around 33 ±1 dB measured in the tunnel. This difference could be explained by the fact that the boundaries conditions are different during the measurements in laboratory and in the tunnel.

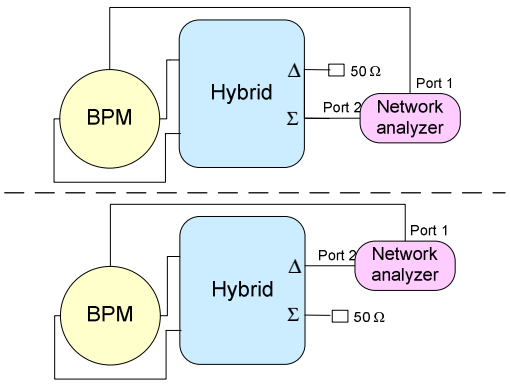

Figure 13. Representation of the cross talk measurement.

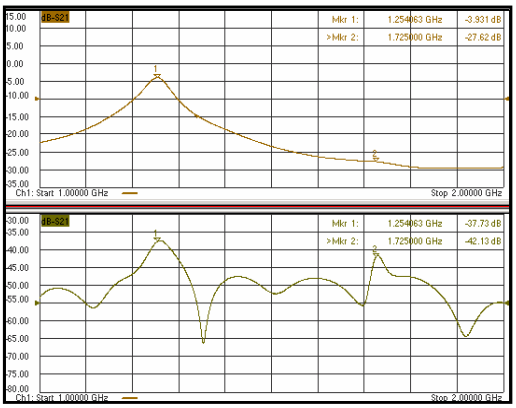

Figure 14. Signal coupled between two antennas positioned at 90°.

Figures 15a and 15b represent the signal measured on one pickup with a 5 GHz bandwidth scope.

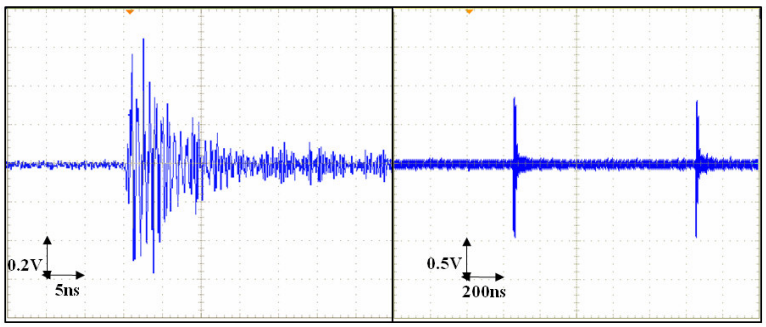

FIGURE 15a & 15b: Signal from one antenna.

Figure 15a represents the same signal than the one in Fig. 15b but the time base is longer. It shows a clean separation between two macropulses distant to 1 µs. No long range echo is observed, confirming the possibility for measurements in a multi-bunch mode.

Figure 16 shows the Fourier transform of a signal on the output of one pickup. The step around 3 GHz fits with the 2.94 GHz cut-off frequency of the beam pipe mode (TM_{01}). The modes, having a frequency above can propagate in the beam pipe. Conversely, the disturbances above the cut-off frequency from elsewhere can also propagate down to the BPM.

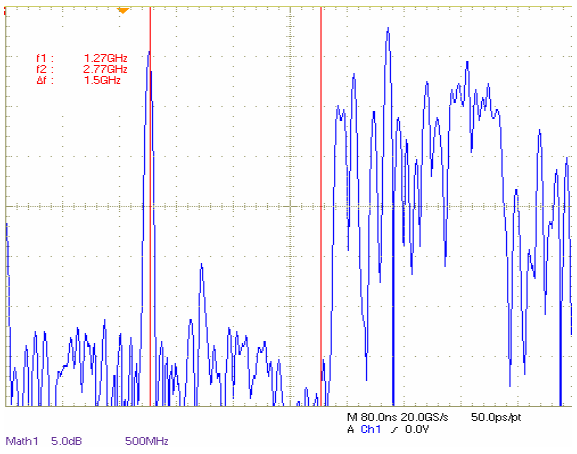

FIGURE 16: Pickup signal spectrum

The transmission measurement on the opposite antennae was completed in the 1 to 4 GHz range (Fig. 17). All peaks correspond to eigenmodes present in the re-entrant cavity. The first and second peaks are the monopole and dipole modes, the others are higher order modes which can propagate out of the cavity through the beam pipe. The 1.72 GHz band pass filter, used in the signal processing, was measured in laboratory and at 3 GHz, its attenuation is around -70 dB and around -60 dB at 4 GHz. These 'higher order modes' should be therefore well rejected.

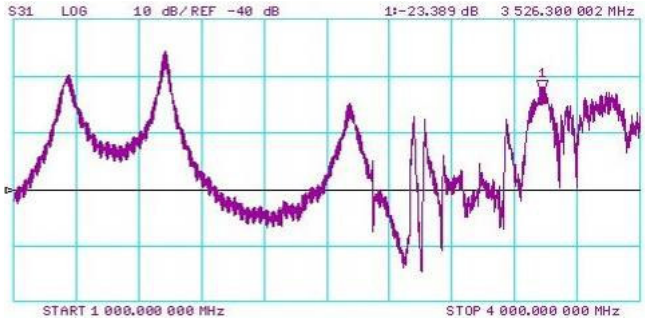

FIGURE 17: Transmission measurement on the two opposite antennas without beam

RF Signal Processing Electronics

The signal processing uses a single stage down conversion to obtain Δ/Σ and is shown in Fig. 18. It is composed of standard RF components: hybrid couplers, phase shifters, filters, isolators and mixers. The lowpass filter behind the mixer has a bandwidth about 60 MHz, which determines the lowest bandwidth in the signal processing.

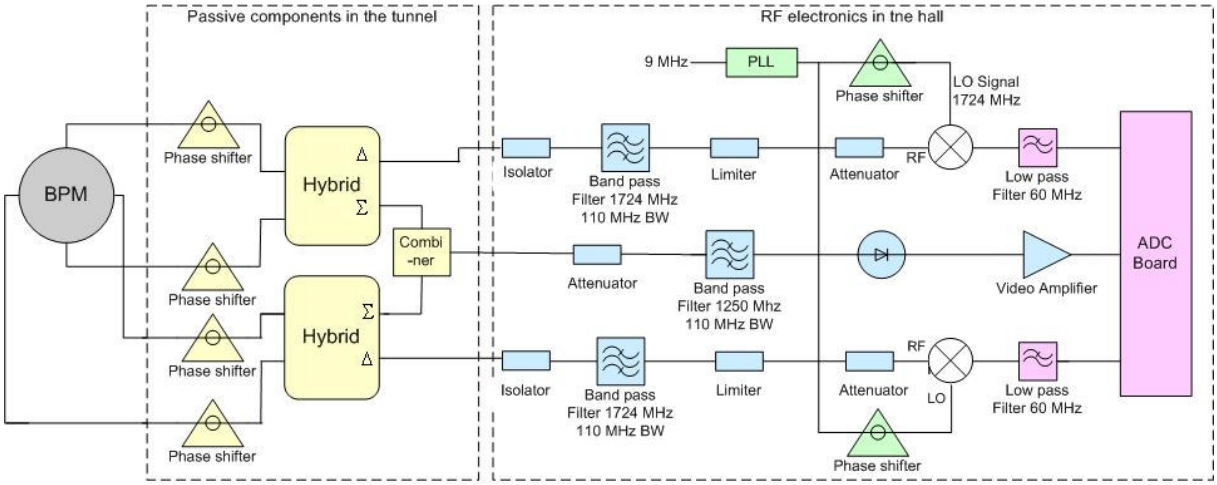

FIGURE 18: RF signal processing electronics

The Δ and Σ signals are obtained from a passive 4-ports 180° hybrid. The 180° hybrid coupler is connected to each pair of opposite antennas with some semi-rigid cables. The rejection of the monopo le mode, on the Δ channel, proceeds in three steps:

- a mode symmetry based rejection with a hybrid coupler. Its isolation is higher than 20 dB in the range of 1 to 2 GHz. A local enhancement of the isolation to be about 30 dB at the frequency of the dipole mode can be obtained with additional external phase shifters and attenuators.

- a frequency domain rejection with a band pass filter centered at the dipole mode frequency. Its bandwidth of 110 MHz also provides a noise reduction.

- a synchronous detection of the dipole mode signal. A 9 MHz reference signal, from the linac control system is combined with a PLL to generate a local oscillator signal (LO) for the mixers at the dipole mode frequency. Phase shifters are used to adjust the LO and RF signals in phase.

The digital electronics, also, makes the sampling, the calibration of the system and the control-command interface. The signal on the Σ channel is used in order to normalize the Δ signal, which determines the position of the beam. This normalization is, also, made by a digital electronics.

Summer 2006, the two subsystems, composing the signal processing, were installed and calibrated:

- a subsystem composed with hybrid couplers, phase shifters and one combiner was installed in the tunnel (Fig. 19) during the maintenance day. The spectrum analysis of the "delta" signals from the 180° hybrid coupler output shows good common mode rejection. Tuning of the phase shifters gives a high common mode rejection (30 dB at 1.25 GHz).

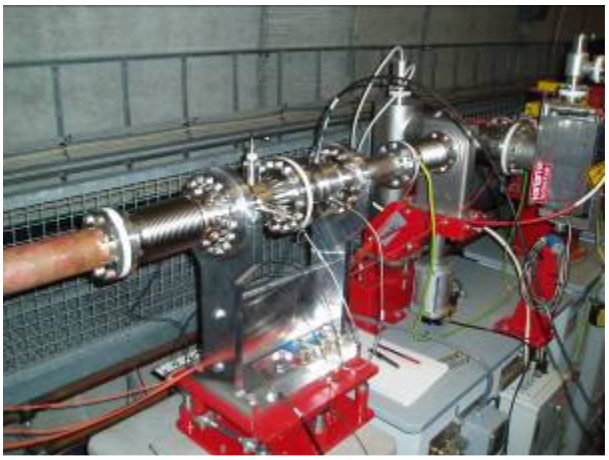

FIGURE 19: Re-entrant cavity BPM and subsystem with hybrid couplers and phase shifters installed in the FLASH linac

- the second subsystem (Fig. 20) was installed in the hall, outside the tunnel. The synchronous and direct detectors, as well as limiters for protection were adjusted to have a linearity range around ± 10 mm.

FIGURE 20: Signal processing electronics located in the hall

The spectrum analysis of the "delta" signals from the 180° hybrid coupler output shows good common mode rejection. Phase tuning for the synchronous detection was refined while visualizing the delta/sigma signal on a scope. The video amplifier gain was adjusted to ± 1 V to avoid saturation from ADCs. Figure 21 shows the signals from video amplifier outputs of Δx and Δy channels.

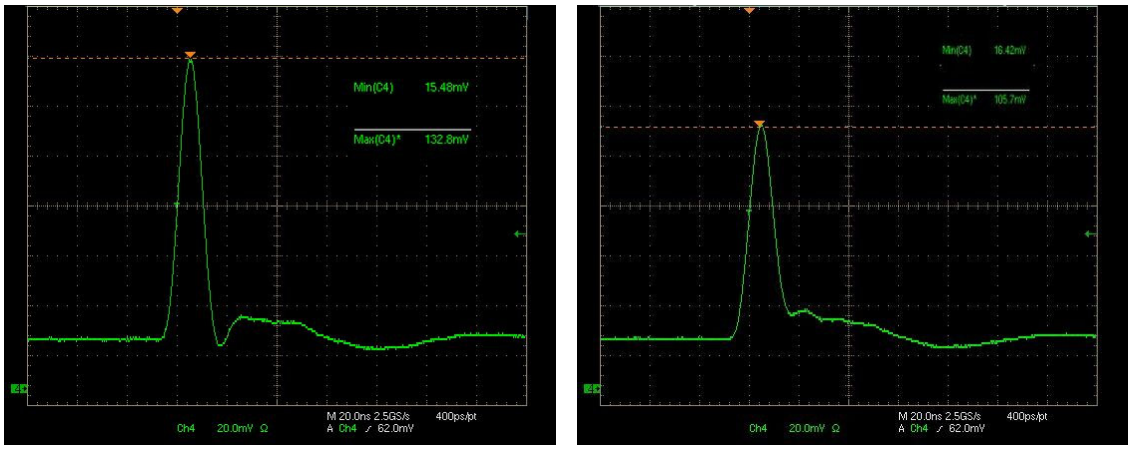

FIGURE 21: Signals at video amplifier outputs, Δx (left) and Δy (right).

Estimation of the performances for different BPM systems

Position Resolution and Offset

The position resolution is the minimum position difference than can be statistically resolved. It is an RMS value related to the signal to noise ratio in the system. The signal voltage of the BPM is determined by the beam's energy loss to the dipole mode and by the external coupling of the coaxial cable.

To assess the performance of the system, a model (cavity+signal processing) is elaborated with a Mathcad code based on Fourier transforms. The simulation covers a span from 0 to 20 GHz. Each mode of the cavity is modeled as a resonant RLC circuit. The delivered time domain signal is therefore determined by the RF characteristics of each mode. The single bunch response of the cavity depends on frequency ω_i and quality factor Q_i of the mode. The signal from a pickup is the sum of all resonant modes excited by the beam.

$$S_{pickup} = \sum S_i \qquad (2)$$

$$S_i = \Phi(t)\left[V_i.\exp\left(-\frac{\omega_i.t}{2.Q_i}\right).\cos\left(a_i.t - \frac{\omega_i.\sin(a_i.t)}{2.Q_i.a_i}\right)\right] \qquad (3)$$

$$\text{with } a_i = \omega_i.\sqrt{1-\frac{1}{4.Q_i^2}} \text{ and } V_i = \sqrt{\frac{\omega_i^2.\left(R/Q\right)_i.q^2.R_0}{\xi_i.Q_i}}$$

where $\Phi(t)$ is the Heaviside function, q the bunch charge, R_0 the 50 Ω cable impedance, R/Q_i defines the coupling to the beam and $\zeta_i = 4$ if it is a monopole mode or $\zeta_i = 2$ if it is a dipole mode.

To simulate the signal processing, the transfer functions of different components are used. A description of the method is given for the Δ channel (Fig. 22).

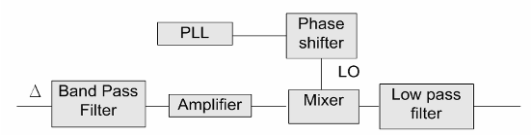

FIGURE 22: Δ channel signal processing

The transfer function of cables (H_c) takes into account the effect of attenuation and dispersion. The length of cables was chosen to be around 33 m. The model of the 180° hybrid couplers composing the signal processing is derived from measurements with a network analyzer: the transmission measurement from the port 1 to port Δ, as shown Fig. 23, gives the transfer function 'Hdiff1', the transmission from the port 2 to the port Δ gives 'Hdiff2'.

The same measurements are made with the port Σ to determine 'Hsum1' and 'Hsum2'.

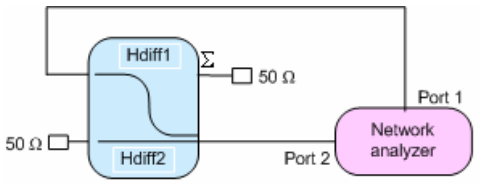

FIGURE 23: S parameters measurement of the hybrid 180°

The hybrid isolation is determined by the following relation :

$$I_{hybrid} = 20 * \log\left(\left|Hdiff1 + Hdiff2\right|\right) \qquad (4)$$

Those hybrid couplers have an isolation higher than 20 dB in the pass-band of 1-2 GHz but are different in details especially outside the pass-band (Fig. 24).

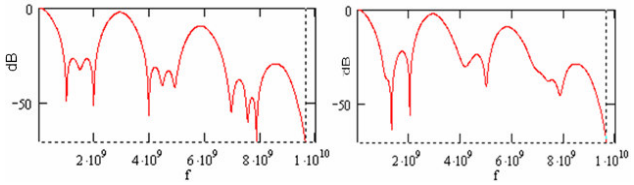

FIGURE 24: Isolation of two 180° hybrid items.

A local enhancement of the isolation can be obtained with adjusting of the phase and attenuation. The Δ signal from the hybrid is given by the following relation:

$$T_\Delta = \left[\left((S_m - S_d).H_c.Hdiff1\right) + \left((S_m + S_d).H_c.Hdiff2\right)\right] \qquad (5)$$

To validate the model, the "sum" signal peak power was measured around 36 dBm for 0.9 nC, it is of the same order of magnitude compared to simulations.

The band pass filter has a 110 MHz bandwidth centred at 1.72 GHz. Its transfer function is given by a CAD code. The filter output signal is the RF signal (Fig. 25a). The local oscillator (LO) signal is modelled by a sine wave at the dipole frequency with 1 Volt amplitude. A phase shift is added to put in phase the LO signal and the RF signal (without monopole mode) from the Δ channel. Follows a 60 MHz lowpass filter, which the transfer function is given by the same CAD code. The IF output signal (with monopole mode) (Fig 25b) is, then, sampled at the peak for a significant beam offset around 10 mm.

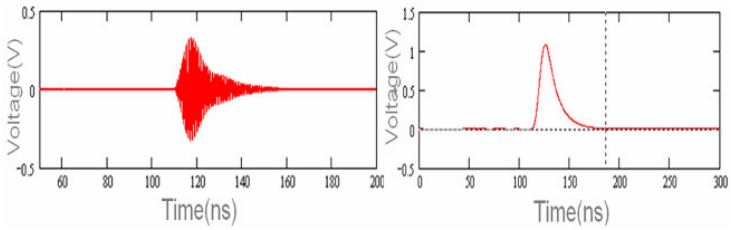

FIGURE 25: RF (a) and IF (b) signals from the Δ channel.

The position resolution is limited by the signal to noise ratio of the system.

The noise comes from the thermal noise and some components used in the signal processing electronics. For the estimation, only the thermal noise, the noise figure and the noise generated in devices are taken into account. The thermal noise of a system is given by the following equation:

$$P_{th} = k_b * T * BW \qquad (6)$$

where k_b is Boltzmann's constant ($1.38*10^{-23}$J/K), BW is defined by the bandwidth of the signal processing channel in Hertz, and T is the room temperature in Kelvin.

The noise level present at the output of the cavity BPMs is amplified by the devices which compose the signal processing electrnics. To calculate the noise level, the thermal noise is added to the noise factor and to the gain. The noise level is therefore given by the following equation:

$$P_n = NF * G * P_{th}. \qquad (7)$$

where NF is the total noise figure of the signal processing channel, G is the gain of the signal processing and P_{th} is the thermal noise. The total noise introduced into the system by the electronics can be evaluated by the noise figure in a cascaded system and is applied by the following formula:

$$NF = F_1 + \frac{F_2 - 1}{G_1} + \frac{F_3 - 1}{G_1 * G_2} + \ldots \qquad (8)$$

where NF is the total noise factor of the signal processing, F_i and G_i are respectively the noise factor and the gain of component i.

As the bandpass filter bandwidth (110 MHz) is larger than the one of the lowpass filter (60 MHz), the thermal noise power is defined by the lowpass filter bandwidth, i.e. BW is equal to 60 MHz in equation 6. The noise amplitude in the hall was measured on the ADC board and on a scope to be about 200 µV peak. The RMS environment noise is therefore around $6.5*10^{-5}$ V that limits the resolution for the re-entrant BPM. As the limitation of the resolution is due to the ADCs noise, to improve the resolution, the dynamic range has to be reduced.

The following table 3 gives the signal behind the low pass filter with 10 mm and 1 mm beam offset, the total noise and the resolution. With a 1 mm beam offset, the signal processing electronics has been modified to get a better resolution, an amplifier with a gain around 18 dB has been added.

TABLE 3. Signal and noise level calculated for the re-entrant BPM

Systems	**Signal on Δ channel (mV)**	**Total noise (mV)**	**Simulated resolution (µm)**
BPM with 10 mm beam offset	181	$6*10^{-3}$	3.65
BPM with 1 mm beam offset	149	$3*10^{-2}$	0.45

Time Resolution

One of the most important parameters for a BPM is the time resolution, which is usually identified to the damping time and is given by the following formula:

$$\tau = \frac{1}{\pi * BW}. \qquad (9)$$

where BW is the bandwidth in Hertz, defined by the relation:

$$BW = \frac{f_d}{Q_{ld}}. \qquad (10)$$

with f_d the frequency and Q_{ld} the loaded quality factor for the dipole mode. For bunch to bunch measurements, the time resolution has to be smaller than the space between bunches of the machine. The time resolution is therefore around 9.5 ns for the re-entrant BPM. It is lower than the separation between bunches on the FLASH linac (110 ns); the bunch to bunch measurements is therefore possible.

In practice, the rising time to 95% of a cavity response signal is 3τ. For bunch to bunch measurements, the time resolution has to be smaller than the distance between bunches ΔT, the system has to verify the following equation:

$$6\tau \leq \Delta T \qquad (11)$$

To evaluate the time resolution of the BPM systems (cavity+electronics), the model is used to simulate the output signal from the synchronous detection. The time resolution is therefore defined by the time interval at 5% of the peak voltage from the baseline.

The length of the signal for the re-entrant BPM behind the signal processing electronics (Fig. 26) was measured around 40 ns. It confirms the possibility to carry out measurements in multi-bunch mode.

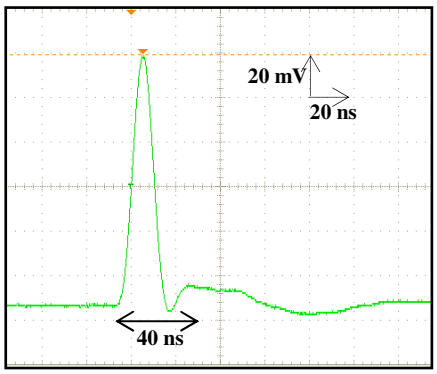

FIGURE 26: Output Signal from the signal processing

First beam tests of the new re-entrant BPM

After the electronics calibration, the first beam tests of the re-entrant BPM, installed in the warm part on the FLASH linac, were carried out. The steerers were used to move the beam, and the magnets between the steerers and the BPM were switched off to reduce errors and simplify calculation. The relative beam position is calculated in using a transfer matrix between steerer and BPM for each steerer setting. An average of 500 points for each steerer setting is put. Our objective was to start the calibration of this BPM, for high precision beam position measurement in single bunch mode with a charge around 1 nC.

Firstly, the deviation range was limited to ±5 mm for a more accurate calibration (Fig. 27).

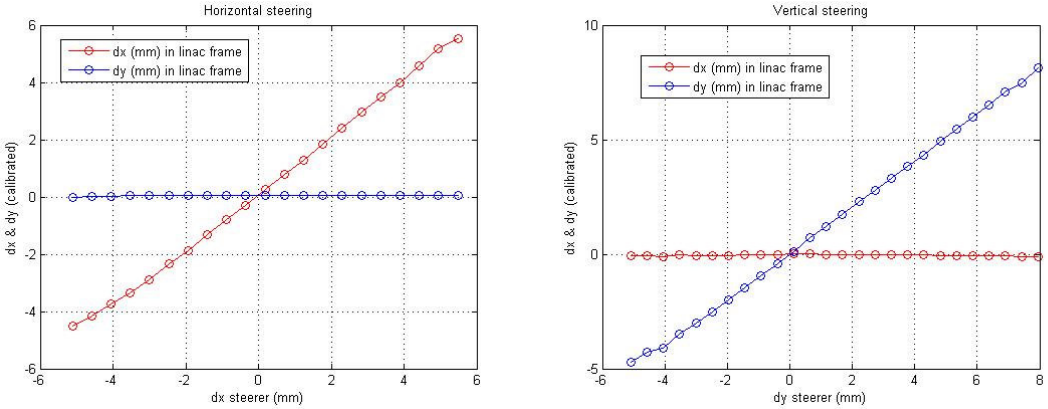

FIGURE 27: Calibration results from horizontal (left) and vertical (right) steering

The linearity in this calibration range ±5 mm is very good for both channels. Then, the standard deviation of the calibrated position measurement was plotted for the horizontal and vertical steerings (Fig. 28).

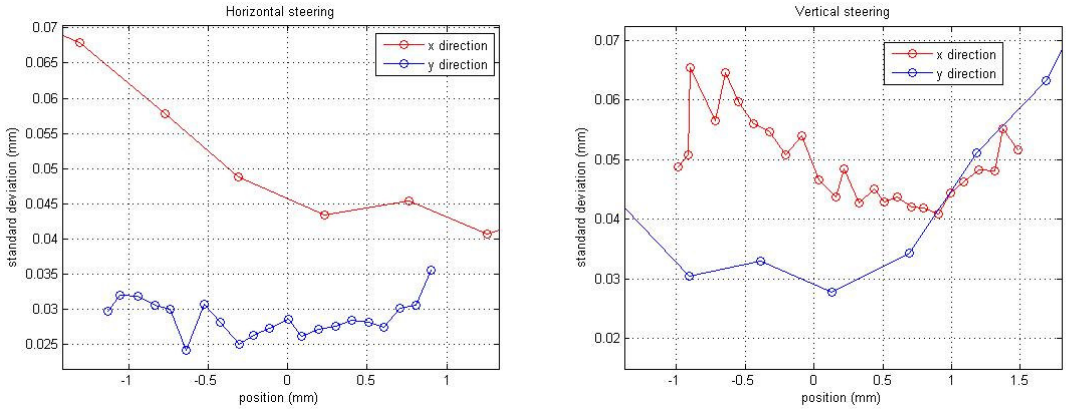

FIGURE 28: Standard deviation of the position measurement (calibrated)

The minimum standard deviation of the measurements at the BPM center is around 40 µm for X channel and around 30 µm for Y channel. But those results depend on the beam jitter, too.

A second test period was necessary to validate the first results, the deviation range was limited to ±10 mm for a more accurate calibration. The position measured by the re-entrant BPM vs. the calculated position was plotted for the horizontal and vertical steerings (Fig. 29).

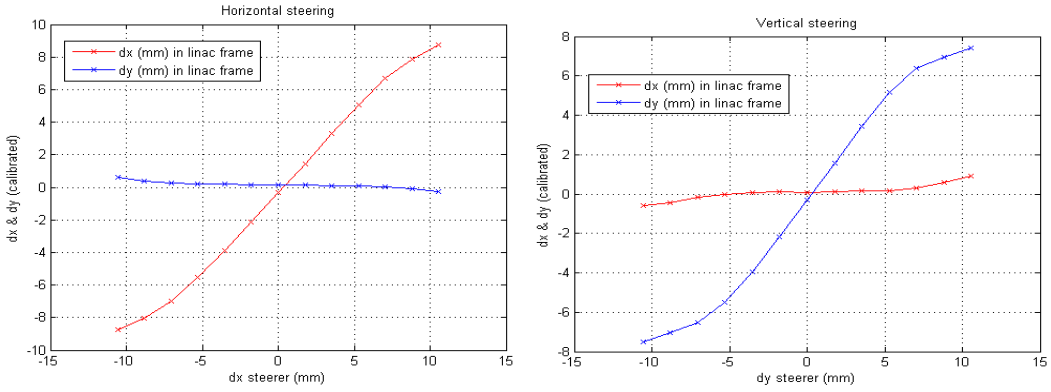

FIGURE 29: Position read by new re-entrant BPM vs. the predicted position from horizontal (left) and vertical (right) steering.

Figure 29 shows a good linearity in a range ± 5 mm. The BPM resolution has been measured by correlating the reading of the re-entrant BPM in one plane against the readings of all other BPMs in the same plane [5]. In keeping the same dynamic range, the resolution was measured, on the Y channel, around 4 µm and on the X channel around 8 µm limited only by the electromagnetic contamination in the experimental hall. Those results are quite similar to the theoretical resolution calculated around 3.65 µm with 10 mm beam offset.

The charge of the re-entrant BPM was calibrated thanks to the toroids and its resolution is around 6.35 pC.

To improve the linearity dynamic range, a 6 dB attenuator was added on each channel. Figure 30 shows the position read by the re-entrant BPM versus the predicted position in horizontal and vertical steerings. With this new configuration, the re-entrant BPM has a good linearity in a range ± 10 mm with a 0.8 nC charge.

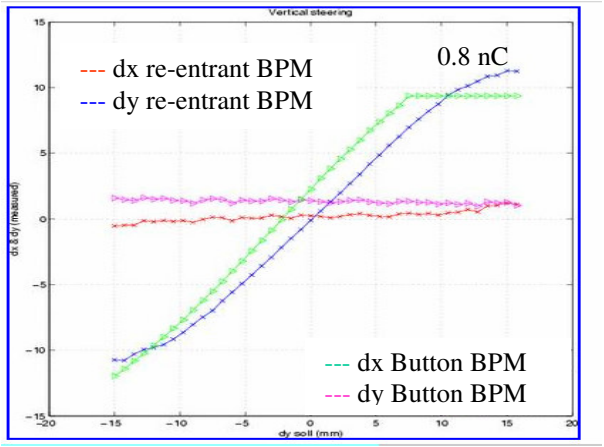

FIGURE 30: Position read by the re-entrant BPM vs. the predicted position in vertical steering with a 0.8 nC charge.

Then, the charge was modified to study the linearity and the resolution of the re-entrant BPM. Figure 31 shows linearity in a range ± 15 mm with a 0.45 nC charge. We suppose that this difference of range linearity between a charge around 0.8 nC and a charge around 0.45 nC, is due to the saturation of the limiter.

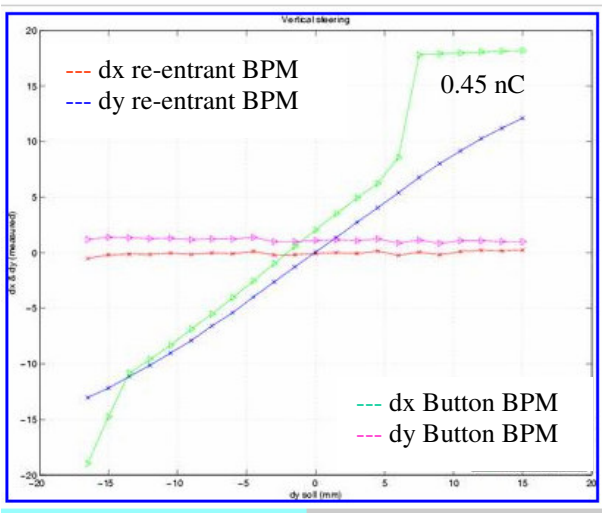

FIGURE 31: Position read by the re-entrant BPM vs. the predicted position in vertical steering with a 0.45 nC charge.

As shown Fig. 30, Fig. 31 and Table 4, in moving the charge, the linearity is always good but the resolution is degraded. Table 4 shows a comparison of the resolution with different values of the charge and between a system with and without 6 dB attenuator.

TABLE 4. Resolution of the re-entrant BPM

Charge (nC)	BPM (µm)	BPM + 6 dB attenuator (µm)
1	~ 4	
0.8		~ 12
0.5	~ 11.8	~ 21
0.2	~ 30.1	~ 55

This BPM was designed to have the possibility to do some bunch to bunch measurements. The position of each bunch can be known and read by the re-entrant BPM as shown on Fig. 32.

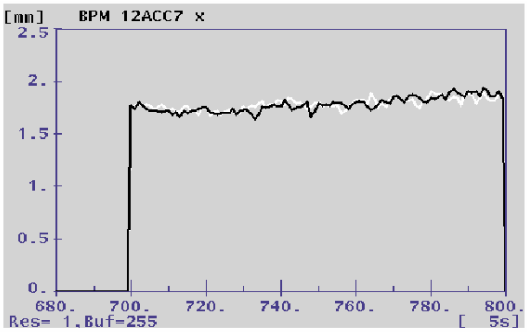

FIGURE 32: Position of 100 bunches in a macro-pulse read by the re-entrant BPM

Conclusion

This BPM is designed to be used in a clean environment, at cryogenic or room temperature. Its main features are the small size of the RF cavity, a large aperture (78 mm) and an excellent linearity. A first prototype has already proved its operation at cryogenic temperature inside a cryomodule, in an environment where dust particle contamination has to be avoided. The second installed on the warm section in the FLASH linac shown a high linearity in the range of ± 10 mm, and high position resolution below 10 µm (4 µm for the Y channel and 8 µm for the X channel) and has the possibility to do some bunch to bunch measurements.

Few dozen of this BPM will be installed in the XFEL cryomodules and it appears, too, as a good candidate for being installed in the ILC cryomodules.

Acknowledgements

We acknowledge the support of the European Community-Research Infrastructure Activity under the FP6 “Structuring the European Research Area” programme (CARE, contract number RII3-CT-2003-506395).

We thank our colleagues from DESY: the TTF operational team for its support, MDI and MVP teams for their help at DESY site and the fruitful discussions on the BPMs. We would like, too, to thank all our colleagues from CEA Saclay for their work on this project.

References

[1] R.Bossart, “High precision beam position monitor using a re-entrant coaxial cavity” Processings of LINAC94, KeK, (1994).

[2] C.Magne, et al., « High resolution BPM for the future linear colliders, LINAC98 Conference, 1998

[3] C Magne, et al, “Reentrant cavity BPM for linear colliders”, BIW2000.

[4] S. Molloy et al, “Measurement of the beam’s trajectory using the higher order modes it generates in a superconducting accelerating cavity”.

[5] N. Baboi, et al., “Resolution Studies at Beam Position Monitors at the FLASH Facility at DESY”, BIW 2006.

[6] C. Simon, et al., “High Resolution BPM for linear collider”, BIW 2006.